

Characterization of the radiation damage in the Chandra X-ray CCDs

G. Prigozhin, S. Kissel, M. Bautz, C. Grant, B. LaMarr, R. Foster, G. Ricker

Center for Space Research,
Massachusetts Institute of Technology,
Cambridge, Massachusetts 02139

ABSTRACT

Front side illuminated CCDs comprising focal plane of the Chandra X-ray telescope have suffered some radiation damage in the beginning of the mission. Measurements of CTI and dark current at different temperatures led us to conclusion that the type of damage is inconsistent with the much studied type of damage created by protons with energies higher than 10 MeV. Intensive ground based investigation showed that irradiation of a CCD with low energy protons (about 100 keV) results in the device characteristics similar to the ones of the flight chips (very low dark current, the shape of the CTI temperature dependence). We were able to reliably determine that only image section of the flight chips was damaged and therefore only fast transfer from image to frame store section was affected. We have developed several techniques in order to determine the parameters of the electron traps introduced into the transfer channel of the irradiated device. One of them is based on the analysis of the amplitude of the signal in the pixels trailing the pixel that absorbed an X-ray photon of known energy. Averaging over large number of photons allowed us to get high signal/noise ratio even for pixels with extremely low signal far behind the X-ray event. Performing this analysis at different temperatures we were able to measure trap density, emission time constant, and trap cross section. Another technique is based on the analysis of the tail behind the events of very high amplitude, such as cosmic ray hits.

We have developed a new scheme of clocking the device which prevents several rows of image section from being ever read out and keeps them moving back and forth. This so-called "squeegee mode" improves CTI and can also be used to measure trap parameters, being especially effective in measuring long time constants.

At least 4 different types of traps were detected, two of them with short time constants in the range from tens to a few hundred microseconds. The most damaging for the device performance are the traps with longer time constant in the millisecond range.

The measurement of the trap parameters allows us to accurately model charge transfer inefficiency and helps to choose optimal operational parameters, and eventually will lead to techniques that may noticeably improve performance of a damaged CCD.

Keywords: Charge Coupled Devices, X-ray spectroscopy, radiation damage, electron traps

1. INTRODUCTION

Soon after Chandra X-ray Observatory was launched into orbit and produced first images of the superb quality, the CCD focal plane was moved out of the focus of the telescope into the position where it could see the on-board calibration source. An analysis of the calibration source data immediately revealed that all of the CCD chips had suffered some damage causing a significant jump in the charge transfer inefficiency (CTI). This triggered the most intensive investigation both of the type of the damage and the reasons that caused it. Originally high energy protons were considered the biggest threat to the Observatory due to their penetrating and damaging properties and also due to their high density in the space environment. Because of that intensive studies were conducted of the CCD damage by protons in the tens of MeV range.²⁻⁵ It became clear very soon, though, that the type of the damage the Chandra devices had experienced is inconsistent with the results obtained in our lab by irradiating the Chandra-like CCDs with 40 MeV and 10 MeV protons. The main difference was extremely low dark current of the flight devices, even when the focal plane temperature was elevated to -50 C. Devices irradiated on the ground showed several orders

Correspondence (G. P.): E-mail: gyp@space.mit.edu, Tel.: (617) 253-7246

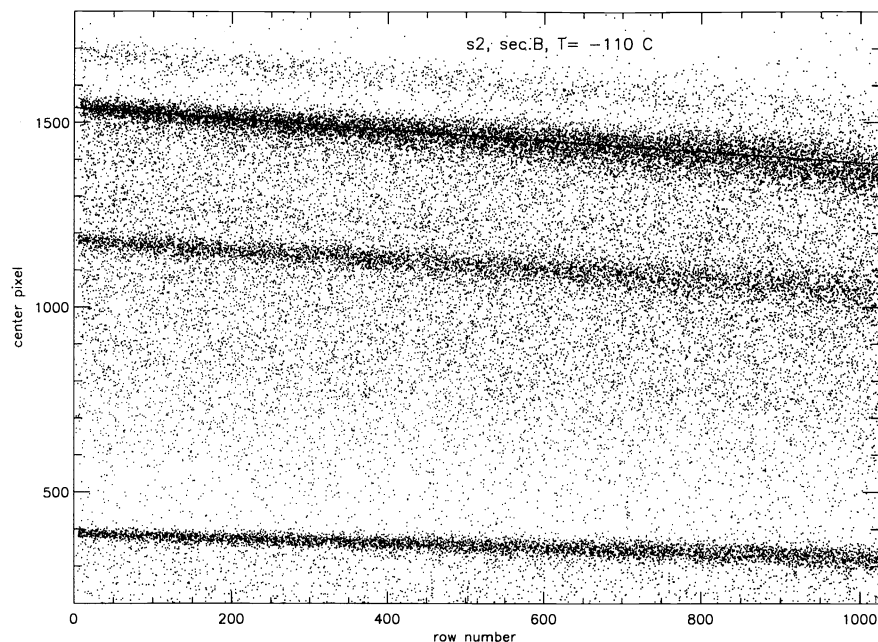


Figure 1. Pulseheight of the center pixel as a function of row number at -110 C for the damaged flight device S2.

of magnitude higher dark current at the same temperature. Also, the dependence of the CTI on temperature looked different for the ground irradiated chips.

We started to look for another type of damaging irradiation which could produce flight-like results. There seem to be no data in the literature on the damage caused by low energy protons (100 – 200 keV) and we implemented a series of experiments irradiating CCDs with low energy protons. The most credible explanation now seems to be that the damage was caused by the low energy protons leaking through the telescope mirror during the radiation belt passages. The detailed discussion of the Chandra radiation environment and the details of the mechanism of the proton penetration through the telescope structure will be discussed in another talk presented at this conference.¹ In this paper in the sections 2,3 we focus on the mechanism of the damage in the CCDs and the techniques we have developed to measure electron trap parameters. In section 4 we describe a squeegee technique which was developed as a method to improve CTI by supplying some fat zero charge to fill the traps. This technique turned out to be a very efficient way to measure trap parameters.

2. CHARACTERIZATION OF THE DAMAGE IN THE FLIGHT DEVICES

One of the most meaningful ways to demonstrate the transfer inefficiency in a CCD is to plot the pulseheight of an X-ray event as a function of row number when the CCD is illuminated with the monochromatic source of X-rays. A typical example of such a plot for the damaged flight device S2 looking at the calibration source is shown in Fig. 1. The focal plane temperature during this measurement was maintained at -110° C. Each dot in this plot represents an amplitude of the center pixel of an X-ray event, pixels adjacent to the center being ignored. Three emission lines can be clearly seen in the source spectrum as areas with the high density of the dots: $Al K$, $Ti K$ and $Mn K_{\alpha}$. Much weaker $Mn K_{\beta}$ can also be observed near the top of the plot. The amplitude of the pulseheight for each of the emission lines gets smaller at the higher row numbers as charge packets lose charge in every transfer from pixel to pixel. In the beginning of the mission each emission line on this plot was absolutely flat, the width of each line also stayed the same across the entire device.

Extremely important feature of this plot is that the pulseheight-vs-row dependence is linear near the bottom of the image section and does not have a roll off or flattening at small row numbers. This is a strong indicator that unlike the image section of the device the frame store section was not damaged. When the frame store is irradiated and electron traps are introduced into its transfer channel, charge packets formed near the bottom of the image section will travel through the empty traps in the frame store section and experience much heavier charge losses than

the following packets which go over the pixels with partially filled traps. As a result pulseheight-vs-row dependence typically curves down at the bottom of the image section in the frame transfer CCDs with both sections irradiated.

Another fact that helped to establish reliably that frame store section was not damaged is that the pulseheight amplitude near the bottom of the image section is the same as it was in the beginning of the flight before the charge transfer quality deteriorated. If the frame store section were damaged, the signal would lose some fraction of charge passing through the damaged section and the amplitude of the signal from bottom rows inevitably would become lower.

The undamaged state of the frame store section and of the serial register became an important clue in the search of the damage mechanism. ACIS focal plane was constructed in such a way that the frame store section of each chip and the serial registers with the output nodes are protected by a gold plated aluminum shield. The shield has varying thickness, with the minimum being 2.54 mm thick. This explains why only image section of the CCD suffered some radiation damage, but it also implies that the spectrum of the damaging irradiation was very soft. It immediately ruled out protons in the tens of MeV range as the source of radiation damage because they would easily penetrate the thin aluminum shield.

Another strong argument in favor of low energy protons is that only frontside illuminated devices in the ACIS focal plane lost transfer efficiency. Two backside illuminated chips did not change. This means that the 40 microns thick substrate of the backside illuminated device was able to stop the flux of damaging particles from hitting the transfer channel of the device on the unexposed surface of the wafer, and sets even stricter limit to the upper value of the radiation particle's energy. Calculations showed that the proton energy have to be lower than 2 MeV in order to be shielded by the substrate. There is also low energy limit to the particle's energy because the protons have to penetrate the optical blocking filter and the polysilicon gates of the frontside illuminated device to reach the buried channel. This requires the proton energy to be somewhat higher than 50–75 keV.

In our attempt to reproduce the characteristics of the flight devices we tried to irradiate the CCDs with electrons, but could not produce enough bulk damage for the CTI values to be consistent with the flight chip results.

Irradiation of the CCD with 102 keV protons brought the desired effect. Device w459c1, manufactured in the same lot with ACIS flight devices, was irradiated at Goddard Space Flight Center Van De Graaf generator with the total dose of 3.6×10^7 protons/cm². During the irradiation the device was kept at room temperature. The dark current stayed very low, two orders of magnitude lower than for the devices irradiated with 40 MeV protons. And most importantly, the temperature dependence of the CTI which reflects a unique blend of electron traps in the transfer channel of the device looks similar for the flight device and the ground irradiated one. CTI as a function of temperature for the flight chip S2 and for the chip w459c1 is plotted on the Fig. 2. The qualitative agreement between flight and ground based data is good, some discrepancy seen in the Figure 2 is expected and can be explained by several factors. One of them is that the dose of proton flux in the ground experiment was based on the estimates of the flight dose and, of course, it is not possible to guess exactly the right number. Another reason is that the proton spectrum in the ground setup was monochromatic, while in space it is relatively broadband. Also, the temperature regime is very different for ground irradiated device and the flight focal plane, which is very important for the defect formation mechanisms. In flight devices are kept cold at -120° C all the time, while on the ground they are kept at room temperature and are cooled down only during measurements. Besides that, the flight chip sees significant level of background irradiation, and it is very difficult to reproduce similar environment on the ground. We made an attempt to simulate cosmic background by placing a strong Co^{60} source close to the CCD during the measurement process. It obviously has a strong effect (see Fig. 2), moving a CTI curve much closer to the flight device data points. But still, the spectrum of the Co^{60} source is very different from the space radiation environment.

To investigate further the details of the damage mechanism we implemented the techniques described below.

3. PARAMETERS OF ELECTRON TRAP IN THE CHANNEL OF THE FLIGHT CCDS

The temperature dependence of CTI can provide an information about the energy trap parameters. The most common technique was described in,^{6,4} but it does not allow to decouple the trap energy level and the trap cross section, thus making trap identification somewhat ambiguous. Besides that, the technique is based on the implicit assumption that the distance between all the X-ray events is always the same, which in reality is not true.

We have developed a technique of measuring trap parameters which is in essence analogous to the DLTS (Deep Level Transient Spectroscopy) – a common way of trap characterization in semiconductor technology. Like in DLTS

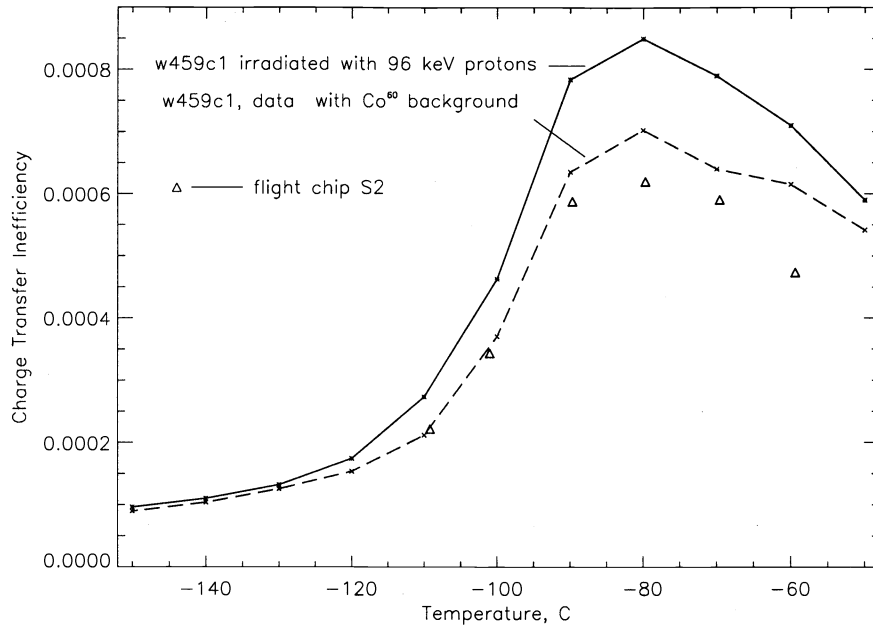


Figure 2. Temperature dependence of CTI for the damaged flight device S2 and device w459c1 irradiated by 102 keV protons.

the traps are filled first and then the detrapping process is observed. Doing that at different temperatures allows to decouple trap energy level and its emission cross section. A valuable feature of the CCD-based technique is that unlike the general DLTS, the location of the sampled traps is restricted to precisely the location of the signal charge in the buried channel, which is an extremely narrow region. Besides that, our technique is much more sensitive and can detect low concentration of traps due to the ability of CCD to detect miniscule amounts of charge transferred over long distances in the bulk of silicon. Our technique of watching the trailing pixels has something in common with EPER technique described long time ago by Janesick,⁷ but is implemented in a different way.

Irradiation of the CCD with protons introduces defects into the transfer channel of the device and these defects act as the electron trapping sites. When signal charge arrives to a pixel potential well the traps inside the volume occupied by electrons will become populated. The usual assumption is that capture time is small compared to pixel storage time and all the traps inside the volume of signal charge get filled. This assumption is very important when calculating the density of traps in the channel, it has no effect though on determining time constants of the trap, which is our major focus at this point. After the charge is transferred into the next pixel the traps start to emit the electrons back into the empty potential well. The same process is repeated for each of the following pixels behind the X-ray event, the integration time for collecting of the reemitted charge is the same for each of the trailing pixels. Thus a tail is formed behind the pixel containing the signal charge. According to the Shockley-Read-Hall theory the detrapping process decays exponentially with time with emission time constant τ_e being determined by the following formula:

$$\tau_e = \frac{\exp(E_t/kT)}{\sigma_t v_{th} N_c}$$

where E_t is energy level of the trap below the conduction band, σ_t is the trapping cross section, v_{th} - thermal velocity of electrons and N_c - effective density of states in the conduction band.

3.1. Tails behind X-ray events

If one looks into the raw frames downloaded from the observatory, there can be clearly seen tails several pixels long behind the X-ray events formed near the top of the frame. The shape of the tail can tell the emission time constant of the trap. Deciphering the time constant may become a tricky business due to the possibility of having several different types of traps with different time constants. Another complication is that signal in the tail behind each individual event is small (especially several pixels behind the event), just a few ADUs, being comparable or smaller than the readout noise of the device. We solved this problem using the power of statistical approach. The trailing

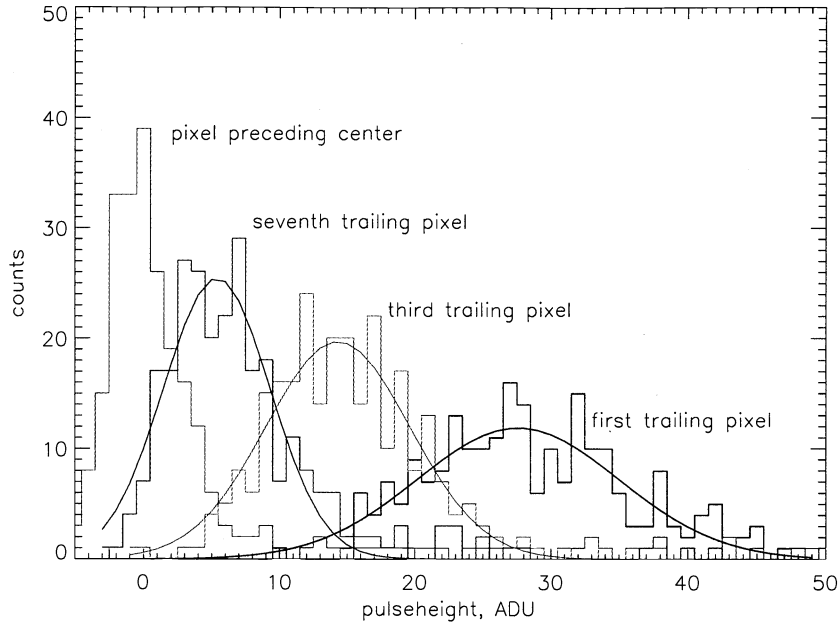


Figure 3. Histograms of the pulseheights in the trailing pixels behind the center of the event. All $Mn K_{\alpha}$ events were selected from the rows above 700. Focal plane temperature -110 C.

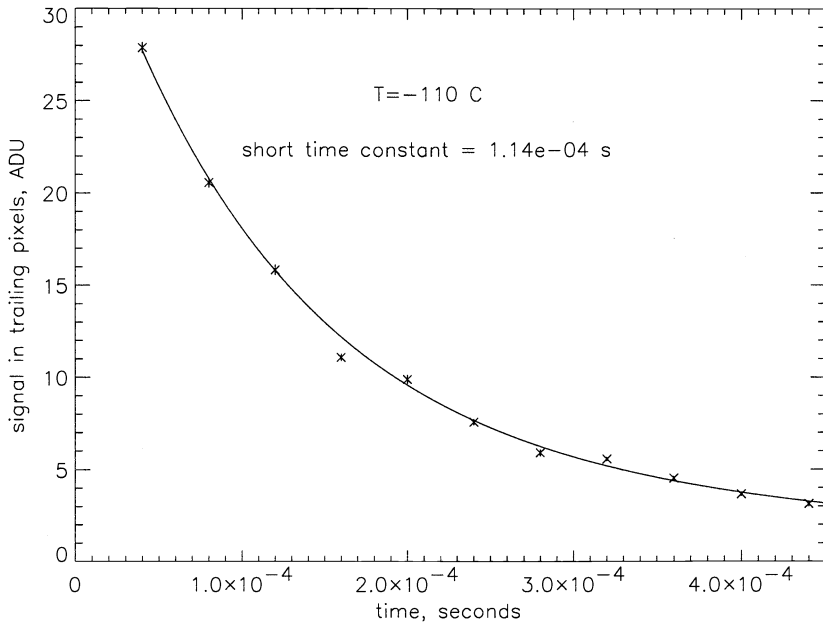


Figure 4. Amplitude of the signal in the trailing pixels as a function of time at focal plane temperature -110 C.

pixel amplitude was averaged over big number of the monochromatic X-ray events originating in the same region of the CCD (and hence undergoing the same number of transfers). The sample histograms of the signal in the trailing pixels are shown in Fig. 3. Histograms of a few trailing pixels are shown, the centers of the histograms shift down for the pixels that are further away. Also shown is a histogram of the pixel in front of the center, and as expected, it is centered around zero. Each of the histograms is then fitted with a gaussian and the centroids of the gaussians are plotted as a function of time behind the central pixel of the event forming the reemitted charge profile. An example of the trailing pixel amplitudes at a focal plane temperature of -110 C is shown in Fig. 4. The amplitudes of the

trailing pixels seem to follow an exponential function very well, the quality of the fit improves dramatically though when two exponentials with different time constants are used. This is a clear indication that there are several types of traps present in the channel of the device. This is not surprising, since experiments described by other workers^{4,5} at higher proton energies indicate multiple energy levels present.

The results of the two-exponential fit suggest that in addition to the time constant of the order of 100 μ s there is another trap with time constant in the *ms* range. We do not show the values for this trap because they cannot be very accurate – making fit to the first 20–30 trailing pixels it is possible to measure only short time constants that have comparable time scale. The longer time constants require a different approach. Still, the densities of both traps could be measured, each of them contribute about 40% to the total charge loss.

The noticeably higher amplitude of the very first trailing pixel in the plot for $T = -115^{\circ}$ C indicates that at low temperatures we start seeing the third trap with yet shorter time constant, which did not come into play at warmer temperatures. But again, the time constant for this trap cannot be accurate, the trailing charge from this trap can be clearly seen only in the very first trailing pixel which is not enough to make a meaningful exponential fit. The density of this trap is small – it accounts for only about 1.5% of the lost charge.

The measurements of the tail indicate that about 20% of the loss is unaccounted for. This means that there must be yet another trap with even longer time constant which could not be detected by this technique. This fact is consistent with the results of “squeegee” technique described below in section 4.

3.2. Tails behind cosmic ray events

The CCDs in the Chandra focal plane experience numerous hits by high energy cosmic particles. Some of them produce signal of a very high amplitude, often saturating the readout circuits. The corresponding amplitude in the trailing pixels after such an event is also very high. These events present another opportunity to measure the time constants of the trap reemission process. Unlike the X-ray events, the amplitude of the signal in the cosmic ray tail stays above noise level for a long time, making it possible to measure long time constant for a single event. In this case it does not make sense to average pixel amplitudes of different traces because the center pixel amplitude is always different for cosmic ray events – they are not monochromatic. Instead, the time constants measured separately for each of the appropriate tails were averaged. At each temperature a fit was made to all available cosmic ray events which had appropriate amplitude and location. The time constants were averaged over all the cosmic rays at a given temperature. The results are shown in the next section on the Fig. 5

3.3. Trap identification

In order to determine trap energy and cross section emission time constants extracted by the techniques described in the previous two sections are presented in the Arrhenius type plot of $\ln(\tau_e T^2)$ as a function of $1/T$ (Fig. 5). According to the theory it should be a linear function, since

$$\ln(\tau_e T^2) = \frac{E_t}{kT} - \ln(A\sigma)$$

where material parameter $A = 1.6 \times 10^{21} \text{ cm}^{-2}$.

It is widely accepted that divacancy is one of the defects introduced into silicon during neutron and proton irradiation. Divacancy is formed when two vacancies generated by irradiation are combined together in a stable immobile complex. The energy level of one of the electron traps associated with it is in the range of 0.2-0.23 eV, according to different sources. The solid line on Fig. 5 represents published divacancy trap parameters ($E_t = 0.21 \text{ eV}, \sigma_t = 6 \times 10^{-16} \text{ cm}^2$) to show that they are close to our experimental results.

Two rectangular points on the Fig. 5 represent the shortest time trap detected at the lowest temperatures (-114.7° and -118.7° C) of the focal plane. The dotted line shows a behavior of the trap with energy $E = 0.16 \text{ eV}$ and cross section $\sigma = 2.1 \times 10^{16} \text{ cm}^2$, parameters that are close to published values for the so called O-V (oxygen-vacancy) trap. This trap is likely to be found in the buried layer of the CCD because near surface layer of the device must be rich in oxygen introduced during the surface oxidation.

We were not able to associate the third trap with slower time constants with any published trap parameters. Our measurements for this trap are the least reliable and this will require further work.

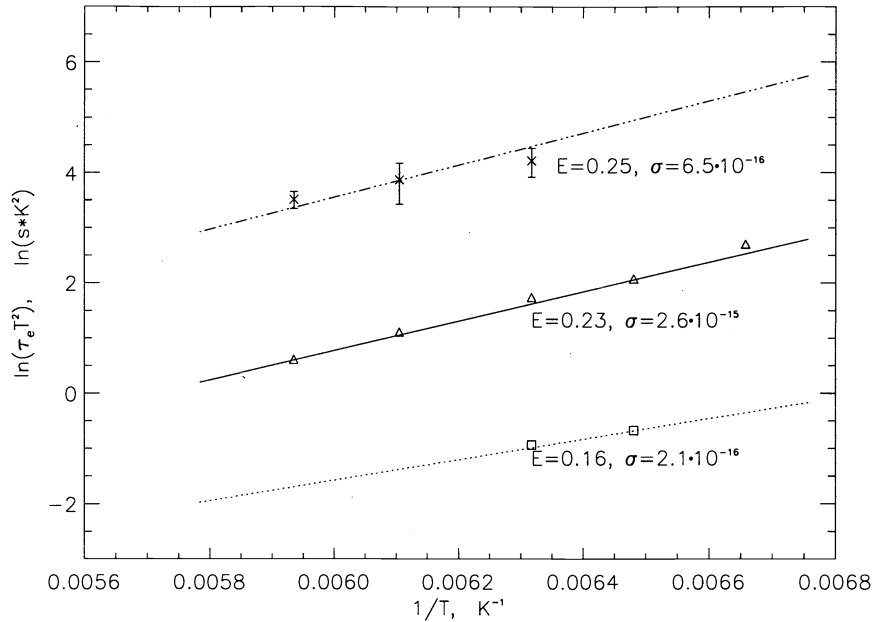


Figure 5. Arrhenius plot of the emission time as a function of temperature.

The most damaging for the device performance is this trap with long time constant in the millisecond range. For this trap the emission time is comparable to the time between events in the same column. As a result the loss of charge in a signal packet depends on the distance to the previous event and this leads to significant loss of the energy resolution near the top of the image section, because the distance between events can vary a lot. This trend is quite obvious in Fig. 1 where the width of each line is noticeably bigger at the end of the frame.

The traps with short time constants also cause the charge loss, but this loss depends only on the number of transfers (in other words, row number). The loss is not a function of prehistory, all the traps are empty when the next charge packet arrives. For such traps it is possible to implement a relatively simple correction algorithm in the processing software and significantly improve the device performance. For the long time constant traps correction is a much more difficult problem because all the previous events have to be taken into account. But still, such a correction can be done if the trap densities and time constants are known. This was a one of the strongest motivations behind the trap parameters measurement.

4. "SQUEEGEE" TECHNIQUE

4.1. Squeegee mode description

There is a population of traps in the buried channel with emission time constants comparable with frame integration time. If such traps are filled in the beginning of each frame, their impact on the X-ray events could be significantly diminished. Significant fraction of these traps will stay filled until the end of integration period and signal charge packets would not lose electrons to them.

In order to utilize this idea a peculiar clocking scheme which we called "squeegee" technique was implemented. Chandra CCDs do not have an input diode to inject charge into the imaging array, so we used particle-generated background to collect charge into the few rows at the boundary of the array. The tests were performed both on the ground irradiated chip and on the flight devices. On the ground a Co^{60} source was placed near the CCD during the testing to produce background charge in the device.

Here is how squeegee mode works. Both sections of the device have 1026 rows. During the fast transfer from image to frame store section the number of transfers was made smaller than the number of rows in the image section. Only $1026 - N_{tr}$ vertical transfers were made, where N_{tr} is a small arbitrary number. This means that N_{tr} rows were left at the bottom of the image section not transferred out. Then, during the slow readout cycle from frame store into serial register the image section was clocked backwards and the bottom N_{tr} rows were shifted to the top

of the array. In the next frame the whole sequence is repeated. Thus, the N_{tr} rows are never read out and after some number of cycles they accumulate enough charge from the particle background to be able to fill the traps in the imaging array in every passage from the bottom to the top.

Flight tests immediately revealed that after the device is turned on in the squeegee mode it takes a very long time (more than an hour) to reach the state of equilibrium in which the bias level of the frame does not change. After the clocking starts the top rows of the CCD immediately below the squeegee rows have significant amount of charge in them, with the amplitude rapidly dropping with increasing distance from the squeegee rows. The amplitude of this excessive charge becomes smaller and smaller in each subsequent frame, until the equilibrium is reached. Where does the charge come from? When the power is off the CCD, the entire bulk of the device is in thermal equilibrium. The n -type buried channel of the device is filled with electrons. Then the clocking starts, and electrons are beginning to be swept out of the buried channel which in normal working state is fully depleted. Normally such cleaning of the CCD array may take a few frames and never is noticed because clocking usually starts before data acquisition. In the case of squeegee mode the situation is different. The squeegee rows keep going up and down the array and are never read out. The potential wells in these rows are filled with electrons to the very top when the power is turned on. In fact they are filled much over the top, but the charge that can spill over the potential barriers separating adjacent pixels will flow into the rest of the array and get swept out.

When the squeegee rows move from the bottom of the frame to the top they fill all the empty traps in every row in the corresponding volume V_{sq} occupied by the squeegee charge. Immediately after the passage of the squeegee packages filled electron traps start to emit charge back into the potential wells. This will form a tail behind the squeegee rows, similar to the tail behind X-ray events (see section 3.1). It is this reemitted charge that forms the signal we see in the top rows of the raw frames in the squeegee mode.

To explain the reduction of trailing signal with time one needs to look into the details of how the squeegee rows lose and replenish their charge.

Every time squeegee rows move down from the top to the bottom of the array they lose charge to fill all the empty traps they meet on their way. Only the traps that are inside the volume occupied by the signal charge are of importance, so the amount of loss is smaller if the signal charge is smaller. During the frame cycle squeegee rows collect electrons generated by all types of irradiation illuminating the device. This is the only source of electrons supply in the squeegee rows and the rate of charge collection is independent of the current signal level. Because of this there must exist an equilibrium level of charge in the squeegee rows that corresponds to the state when the rate of electron loss is equal to the rate of replenishment. Obviously, the level of equilibrium is much lower than the full well condition in the beginning of the run, and that is why the signal level continues to drop during the initial phase.

There are two distinct components of the electron replenishment mechanism. One is the charge accumulated in the squeegee rows while they sit at the top of the array during the integration time. This component is distributed uniformly among all the squeegee rows. For the raw frames in one of the flight tests (the SqueegeeIII test) the total amount of charge generated in the entire CCD array (averaged over many frames) was determined. The resultant charge accumulation rate is $4.636 \text{ ADU}/\text{pixel}/\text{exposure} = 1.449 \text{ ADU}/\text{pixel}/\text{second}$ (one exposure is 3.2 seconds). This results in the 74 ADU of charge accumulated in the 16 squeegee rows during the frame integration time.

Another contribution comes from the charge generated anywhere above the squeegee rows during their shifting down, staying at the bottom, and shifting back to the top. The channel stop region above the very top row of the CCD is an analogue of the concrete wall that reflects ocean waves back into the sea. The channel stop potential is zero, while potentials under the CCD gates are positive, thus all the electrons that were accumulated above the squeegee rows will not be able to move above the topmost row of the CCD when the squeegee rows are being transferred upwards from the bottom of the array. They will be reflected back from the potential wall at the top of the device and will all end up in the first top row of the 16 squeegee rows. If the first row is filled up, the extra charge will spill down to the next row, and the next, and so on. While the time interval corresponding to squeegee rows staying at the bottom is short, the area of charge accumulation is huge - all the 1024 rows of the CCD. Because of that such mechanism plays a significant role in the charge collection. With the standard squeegee timing this component contributes about 60 ADU to the total accumulated charge (calculated assuming the same electron generation rate as mentioned above). What's important, the replenishment of the squeegee rows happens preferentially from the top, while the charge loss is dominant at the bottom row. As a result, in equilibrium most of the squeegee charge must be kept in the topmost of the 16 rows. This speculation was confirmed by the lab experiment where the content of the squeegee rows was read out after running a squeegee mode for a prolonged period of time.

By changing amount of time the squeegee rows stay at the bottom of the image section it is possible to vary the amount of charge accumulated in the squeegee rows. This means that one can decrease the number of squeegee rows and have the same amount of charge by increasing the deadtime (time that squeegee stays at the bottom).

In order to avoid bias frame drift during the initial transition period of reaching the equilibrium, flushing of the entire array was implemented. The electron charge was clocked out of the CCD in a regular operation mode and only after that squeegee mode was turned on. This reduced the transition period to a very short interval and eliminated bias instability.

4.2. The model of the tail behind the squeegee rows.

On its way from the bottom of the frame to the top the squeegee charge fills all the traps in a volume it occupies. Let's assume that squeegee charge leaves Q_0 traps filled in each pixel. If trailing pixel is i rows behind the squeegee row, then by the time trailing pixel reaches the pixel where the squeegee charge was iT seconds ago ($T = 40\mu s$ is the clock period of the fast parallel transfer) only $Q_0 \exp(-iT/\tau)$ traps will stay full. So, during one period of parallel transfer from the bottom to the top the trailing pixel will collect the charge emitted by these traps in the amount of $Q_0 \cdot \exp(-iT/\tau) \cdot (1 - \exp(-T/\tau))$. Here τ is the time constant of one particular trap type. Of course, we will have later to sum over all the different trap types. When the squeegee row arrives to its final position at the top of the frame at row R (counted from the bottom), the pixel i rows behind underwent $(R - i)$ transfers and collected charge

$$Q_0 \cdot (R - i) \cdot \exp(-iT/\tau)(1 - \exp(-T/\tau))$$

After that the integration starts and during the integration time T_{int} the pixel will collect additional reemitted charge which equals to

$$Q_0 \exp(-iT/\tau) \cdot (1 - \exp(-T_{int}/\tau))$$

Finally, the total charge $Q(i)$ in the pixel i rows behind the squeegee row can be described by the following expression (for one trap only):

$$Q(i) = Q_0 \cdot \exp(-iT/\tau) \cdot [(R - i)(1 - \exp(-T/\tau)) + (1 - \exp(-T_{int}/\tau))]$$

This model does not take into account distortions introduced by the charge losses during the transfer of the accumulated charge down from the image section into the frame store. Charge packets in the adjacent rows do not differ much from each other and this should make the distortion of the signal shape due to the CTI small. Also, we did not take into account loss of charge in the squeegee rows themselves while they moves across the frame.

4.3. Extraction of time constants

The model described above was applied to fit the amplitude of the signal in the bias frame with the 16 squeegee rows. No flushing of charge was performed prior to the start of the squeegee mode. Each quadrant was analyzed separately. A histogram of the pulseheights was made for each row. The centroid of the histogram is plotted on Figure 6 as a function of row number behind the squeegee rows. The histogram σ 's are not shown, they were fed as weights into the fitting routine, though. Three different types of traps were assumed, which means that the model had 6 free parameters - a pair of amplitude Q_0 and time constant τ for each trap. The dash-dotted line on the plots represents the best fit model. The quality of the fit looks very good. The corresponding values of τ are shown on each of the plots. Also shown on the plot is the sum of the amplitudes in the all the trailing pixels calculated separately for each of the exponential terms. This number corresponds to the total charge loss related to a particular trap. Two shorter time constants determined this way are similar to the results from other techniques (see sections 3.1, 3.2). The longer time constant could not be measured by other techniques

The same measurement was performed on the ground irradiated device w459c1. Result is shown on Fig. 7. The shortest and the longest time constants seem to be close to the ones measured for the flight device. The millisecond time constant seems to be different, but it is not measured very accurately, because the amplitude of this trap is very low. Significantly different, though, is the relative weight of the traps in this chip. Short trap dominates over the millisecond trap, unlike in the flight chip. This is reflected in the shape of the signal curve - in Fig. 7 it consists mostly of two linear pieces - in logarithmic scale this means that there are two prominent traps, the third one being relatively small. This is not the case for the flight chips signal shape. The above result indicates that the defect

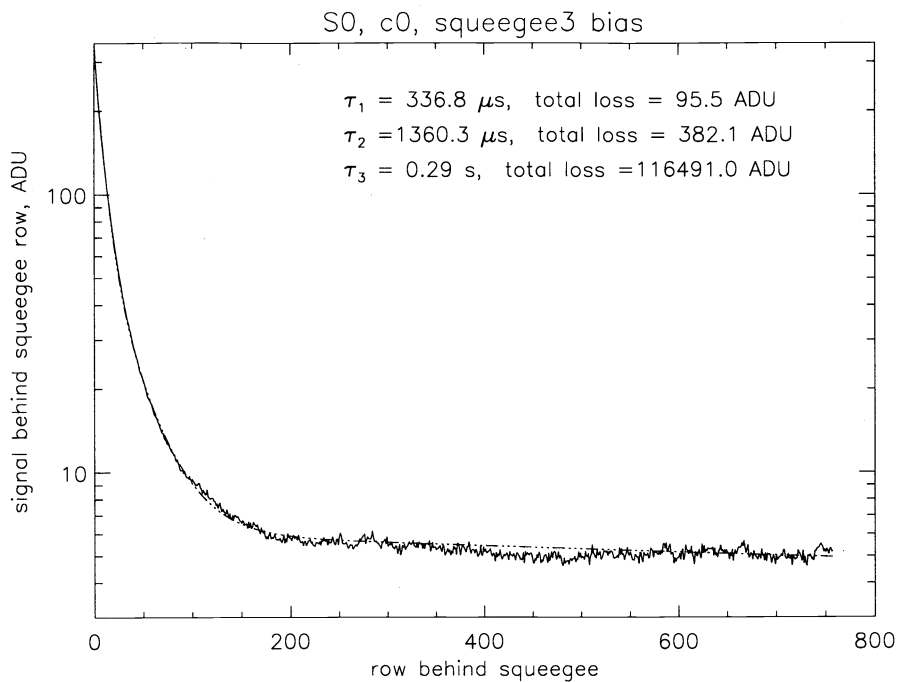


Figure 6. Signal in the trailing pixels behind the squeegee rows. Flight chip S0, quadrant c0. Bias frame with no flush prior to squeegee.

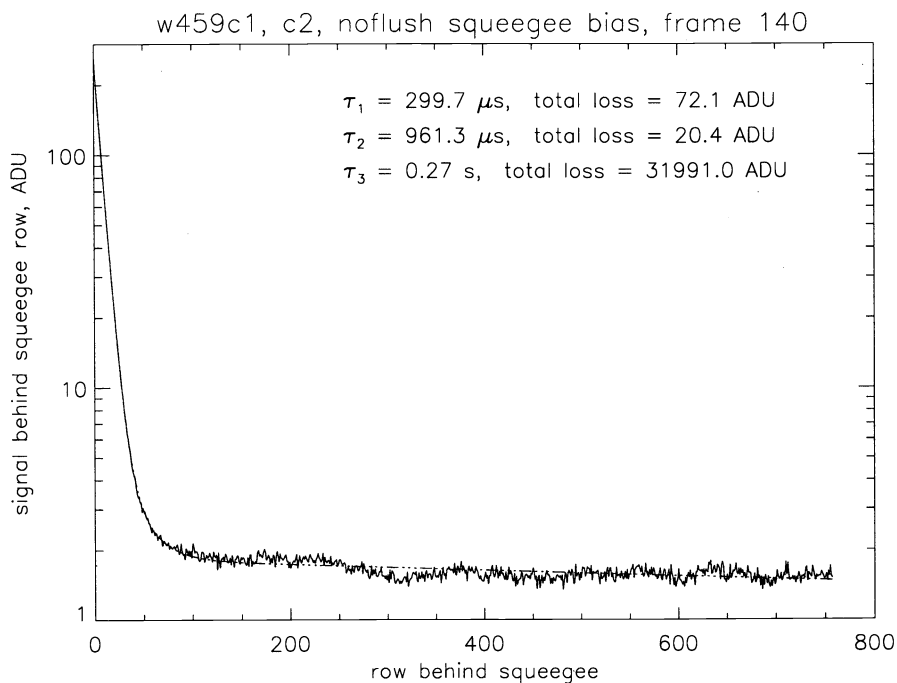


Figure 7. Signal in the trailing pixels behind the squeegee rows. Device w459c1, 15 frames averaged together after frame 140. No flush prior to squeegee.

composition is not identical for the flight devices and the ground irradiated chip. This is not surprising given the differences in thermal treatment and different spectrum of irradiation for both devices.

On Fig. 8 is shown the effect of squeegee mode on the performance of the ground irradiated device w459c1. As

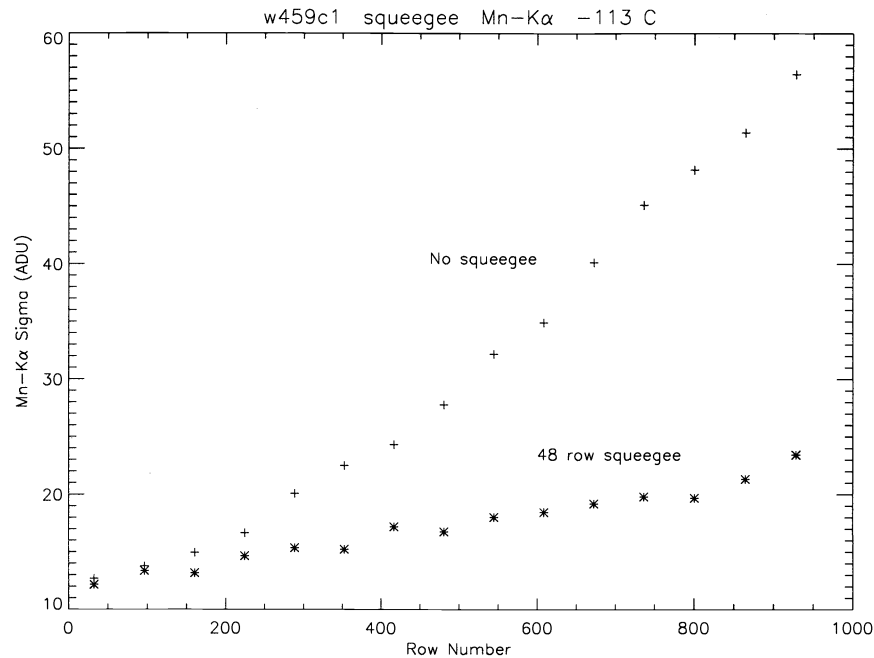


Figure 8. Full width half maximum of the $Mn K_{\alpha}$ peak as a function of row number for the data with “squeegee” and regular clocking.

usual, Fe^{55} radioactive source was used to measure the CTI of the device. The plot of the full width half maximum (FWHM) of the $Mn K$ line as a function of row number for the data taken with and without “squeegee” clocking reflects significant improvement introduced by squeegee mode. The number of accumulating rows in this case was 48. At the top of the array the reduction of the FWHM is more than by a factor of 2, which is a remarkable improvement.

This technique is very efficient in improving the energy resolution of the device, while improvement in CTI is very modest. “Squeegee” technique suppresses the traps with time constant longer than frame time and we showed before that such traps are responsible for about 20% of the charge loss. Because of that it does not have strong effect on the CTI. On the other hand, the same traps are mostly responsible for the loss of energy resolution because the charge loss to these traps changes depending on the distance to the previous event. This seems to be a promising technique which may noticeably mitigate radiation damage effects in the flight devices.

5. CONCLUSION

We have analysed radiation damage in the frontside illuminated CCDs comprising Chandra focal plane. We have developed several techniques for radiation damage characterization and trap parameters measurement. These techniques allowed us to measure trap emission time constants. The damage characteristics are consistent with the type of damage we observed on the ground after irradiating similar chip with low energy (102 keV) protons. We were able to determine that the frame store sections of the flight devices remained intact which is also consistent with the low energy proton hypothesis. We have developed a peculiar clocking scheme (“squeegee” mode) which noticeably improves device performance by filling traps with long time constants in the beginning of each frame. This technique serves also as a powerful method to measure trap time constants. Using this and other techniques we were able to determine that there are at least four different trap energy levels in the flight devices. Similar trap levels were measured on the ground irradiated devices, although the relative densities of the defects seem to differ from the flight CCDs.

6. ACKNOWLEDGEMENTS

This work was funded by NASA under the contract NAS-37716.

REFERENCES

1. S. L. O'Dell, M. W. Bautz, W. C. Blackwell, Y. M. Butt, R. A. Cameron, R. F. Elsner, M. S. Gussenhoven, J. J. Kolodziejczak, J. I. Minow, D. A. Swartz, A.F. Tennant, S. N. Virani, and K. Warren, "Radiation environment of the Chandra X-ray Observatory" SPIE meeting, San Diego, 2000, submitted
2. K.Gendreau, G.Prigozhin, R.Huang, M.Bautz,"A technique to measure trap characteristics in CCD's using X-rays", IEEE Transactions on Electron Devices, v. 42, No. 11, pp. 1912-1917, 1995
3. K.Gendreau, M.Bautz, G.Ricker, "Proton damage in X-ray CCDs for space applications: Ground evaluation techniques and effects on flighe performance", Nuclear Instruments and Methods in Physics Research, A, v.335, pp.318-327, 1993
4. A. Holland,"The effect of bulk traps in proton irradiated EEV CCDs", Nuclear Instruments and Methods in Physics Research, A, v.326, pp. 335-343, 1993
5. T.Hardy, R.Murowinsky, M.Deen,"Charge transfer efficiency in proton damaged CCD's", IEEE Transactions on Nuclear Science, vol. 45, No.2, Apr. 1998, pp.154-163
6. C. Dale, P.Marshall, B.Cummings, L.Shamey, A.Holland, "Displacement damage effects in mixed particle environments for shielded spacecraft CCDs", IEEE Transactions on Nuclear Science, vol. 40, No. 6, pp. 1628-1636, Dec. 1993
7. J.Janesick, G.Soli, T.Elliot, S.Collins,"The effect of proton damage on charge-coupled devices", Proc. SPIE, vol. 1447, pp.87-108, 1991